SCIENCE CHINA
Physics, Mechanics & Astronomy

• Research Paper •

August 2011 Vol.54 No.8: 1481–1487
doi: 10.1007/s11433-011-4393-y

The interfacial fracture behavior of foam core composite sandwich structures by a viscoelastic cohesive model†

SUN ShiYong[1,2] & CHEN HaoRan[1*]

[1]*State Key Laboratory of Structural Analysis for Industrial Equipment, Dalian University of Technology, Dalian 116024, China;*
[2]*Key Laboratory for Precision and Non-traditional Machining Technology of Ministry of Education, Dalian University of Technology, Dalian 116024, China*

Received July 30, 2010; accepted March 18, 2011; published online June 30, 2011

A sandwich beam model consisting of two face sheets and a foam core bonded by a viscoelastic adhesive layer is considered in order to investigate interfacial fracture behavior. Firstly, a cohesive zone model in conjunction with a Maxwell element in parallel, or with a Kelvin element in series, respectively, is employed to describe the characteristics of viscoelasticity for the adhesive layer. The models can be implemented into the implicit finite element code. Next, the parametric study shows that the influences of loading rates on the cohesive zone energy and strength are quite different for different models. Finally, a sandwich double cantilever beam model is adopted to simulate the interface crack growth between the face sheet and core. Numerical examples are presented for various loading rates to demonstrate the efficacy of the rate-dependent cohesive models.

viscoelasticity, interfacial crack, rate-dependent cohesive model, composite sandwich beam

PACS: 46.35.+z, 68.35.-p, 46.50.+a

1 Introduction

Presently, composite sandwich structures with thin, high stiffness face sheets and thick, low density cores are being widely used in weight sensitive structures, such as marine, transportation, civil construction and aerospace applications. The sandwich interface, which transfers stresses and other structural responses between the face sheets and core, is a typical adhesive material with viscoelastic characteristics. The performance of the interfacial layer has a significant influence on the physical, chemical and mechanical properties (as well as the service life) of the composite sandwich structures. As for structures of all dissimilar materials, the interfacial debonding between the core and face sheets is one of the more common failure modes during the processes of initial sandwich manufacturing, in-service under normal and accidental loads. The interfacial crack initiation and growth affects transfer of mechanical responses between the face sheets and core. Furthermore, static and dynamic loading are both likely to inflict unstable crack growth and lead to overall failure; however, due to the anisotropy and non-homogeneity of composite sandwich structures, the analysis of that interfacial failure mode is quite complex [1].

Since the mechanical behavior and failure modes of the interface have a significant influence on the structural performance of sandwich structures, a thorough understanding of the factors that are relevant to the face/core debonding is crucial to the safe design of sandwich structures; therefore, many scholars have devoted their efforts to the interfacial failure behavior of sandwich structures. The influence of an initial through-the-width face/core debonding on the compression failure of the sandwich was examined experimentally by Vadakke and Carlsson [2]. Avilés and Carlsson [3] presented their beam models for the analysis of compliance and energy release rates of the sandwich double cantilever

*Corresponding author (email: chenhr@dlut.edu.cn)
† Recommended by WANG JianXiang (Editorial Board Member)

beam specimens. Sirituk et al. [4] devised an experimental procedure to evaluate the values of delamination toughness at the face/core interface of a sandwich structure for both dry and wet cases. The J-integral computed by the finite element method agrees with the values of their experimental data.

The Cohesive Zone Model (CZM), which is based on the concepts first discussed by Dugdale [5] and Barenblatt [6], has been used extensively to study the fracture and crack growth problems of metals, composites and concrete [7]. Recently, combined with finite element methods, more complicated cohesive laws were developed to simulate interfacial delamination propagation [8]. Sridharan and Li [9] compared two types of CZMs: one with a finite thickness and the other with zero initial thickness. Both static and dynamic delamination problems were simulated. Han et al. [10] used a cohesive element approach to simulate delamination propagation between the face sheets and core in a honeycomb-core composite panel. The critical energy release rate and peak strength of the CZM were determined by Double Cantilever Beam (DCB) fracture tests and Flat-Wise Tension (FWT) tests, respectively.

In the aforementioned literature, the cohesive law is rate-independent; namely, the tractions within the cohesive zone depend only on the crack surface opening displacement, and are independent of the crack opening displacement rate. However, most engineering materials, including polymers and high-temperature metals, are known to creep under sustained constant loads and relax while being subjected to a constant strain. For sandwich structures, face/core debonding within the adhesive layer is rate-dependent because of the viscoelastic behavior of the polymer adhesives. Recently, more and more studies have employed viscoelastic CZMs for polymers in a series of papers [11–16]. For instance, a rate-dependent CZM based on a viscoelastic analyses on the crack-tip process zone was proposed by Bažant and Li [11], in which the traction relates to the effective displacement and rate of change of effective displacement. Allen and Searcy [12] developed a damage evolution law for a nonlinear viscoelastic cohesive zone to reasonably simulate rate-dependent viscoelastic damage growth. As the viscoelastic property matrix is significant for PBX explosives, the rate-dependent CZM was successfully employed in the interface debonding [13]. In addition, comprehensive experimental and numerical studies have been reported in two separate papers by Xu et al. [14,15]. Zhu et al. [16] obtained mode I and mode II traction–separation laws for polyurea/steel sandwich specimens. Strong rate-dependent effects were found for both modes of fracture. The cohesive energy (i.e., fracture toughness) increases with rising crack opening velocity, which is the basis of most rate-dependent CZMs available in the aforementioned literature.

The commonly-used rate-independent CZM has proven to be a suitable and simple model in many cases for fracture analysis [17]. However, for a viscoelastic interface, it may not be adequately precise in some situations [18]. Viscoelastic interfacial crack growth analysis is rare for lack of effective experimental and numerical methods. In this study, two kinds of rate-dependent CZMs are established to characterize the different effects of loading rates upon interfacial viscoelasticity. Furthermore, the interfacial delamination propagation between the face and the core of a sandwich double cantilever beam is simulated using the finite element method. Some conclusions are reached based on the numerical results, which should contribute to better understanding of the interfacial failure mechanisms of composite sandwich structures.

2 Cohesive zone model

An arbitrary crack system, including a cohesive zone in front of the crack tip and the separated upper and lower surfaces, is shown in Figure 1(a) [5,6]. The "fictitious" crack is divided into two parts: one corresponds to the physical length of the stress-free crack; the other one is the cohesive zone, where damage of the material occurs and finite cohesive tractions follow a certain law: including linear, bilinear, parabolic and exponential laws, etc. A classical bilinear softening law for the cohesive zone is illustrated in Figure 1(b) [19]. The cohesive zone usually has two distinctive regions. The first region is defined from points A to B, where material hardening occurs; therefore, point A is assumed to have low magnitude traction. Point B reaches the maximum traction (i.e., cohesive strength) T_m, which is one of the fracture parameters. The second region is defined from points B to C, where material softening occurs. Another fracture parameter, called critical separation δ_c, is defined at point C, where the cohesive traction is numerically negligible. The area under the T-δ curve represents the cohesive energy G_c: namely, the fracture toughness of the material.

The CZM is usually implemented in the finite element approach by a cohesive element [9,20]. The cohesive element, which has zero initial thickness in the un-deformed configuration, can model the interface delamination between continuum elements. Elements in the model are 4-noded, with two displacement degrees of freedom per

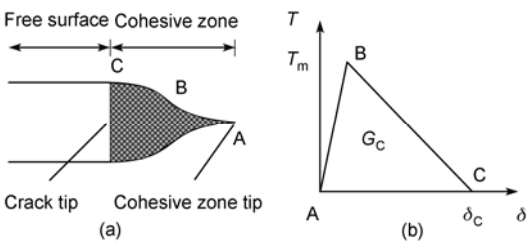

Figure 1 Schematic of a cohesive zone ahead of a crack tip (a) and a typical bilinear softening cohesive law (b).

node for 2D. The relative displacements of the nodes are used to characterize the deformation, and damage occurs only in the cohesive elements which obey the constitutive relation, such as in Figure 1(b).

The opening of the interface element is defined as the difference in displacements between the top and bottom nodes:

$$\Delta u = \{u\}^{\text{top}} - \{u\}^{\text{bot}}. \tag{1}$$

So, the definition of the interface opening Δu_n in terms of the nodal displacements of paired nodes is:

$$\Delta \boldsymbol{u}_n = \boldsymbol{\Phi} \boldsymbol{d}_n = (-\boldsymbol{I}_{4\times4} \mid \boldsymbol{I}_{4\times4})\boldsymbol{d}_n, \tag{2}$$

where d_n is the nodal displacement in the global coordinate system and I is the unit matrix. The node relative displacement vector in the element is then given by:

$$\Delta \boldsymbol{u}(\xi) = \boldsymbol{H}(\xi)\Delta \boldsymbol{u}_n = \boldsymbol{H}(\xi)\boldsymbol{\Phi}\boldsymbol{d}_n = \boldsymbol{B}\boldsymbol{d}_n, \tag{3}$$

where, ξ is the local coordinate of the element with $-1 \leqslant \xi \leqslant 1$. $H(\xi)$ is the matrix containing the shape functions. The nodal force vector and tangent stiffness matrix are defined as:

$$\boldsymbol{f}_N^{\text{el}} = W\int_{-1}^{1} \boldsymbol{B}^{\text{T}}\boldsymbol{\Theta}\boldsymbol{t}_{\text{loc}} \det \boldsymbol{J} \text{d}\xi, \tag{4}$$

$$\boldsymbol{K}^{\text{el}} = -\frac{\partial \boldsymbol{f}_N^{\text{el}}}{\partial \boldsymbol{d}^{\text{el}}} = -W\int_{-1}^{1} \boldsymbol{B}^{\text{T}}\boldsymbol{\Theta}\boldsymbol{D}_{loc}\boldsymbol{\Theta}^{\text{T}}\boldsymbol{B} \det \boldsymbol{J} \text{d}\xi, \tag{5}$$

where W is the width of the interface element; Θ represents the matrix of direction cosines transforming the local coordinate system to the global one; t_{loc} is the cohesive traction vector; det J is the Jacobian determinant; $\boldsymbol{D}_{\text{loc}}$ is the stiffness matrix.

3 Constitutive relation of the rate-dependent cohesive zone model

3.1 Model description

A rate-dependent CZM of the viscoelastic interface of sandwich structures seems to be a reasonable approach to capture the fundamental viscoelastic fracture behavior. Two kinds of three-parameter solid models are employed to describe the viscoelastic nature of the interface. In the case shown in Figure 2(a), the constitutive relation can be written as:

$$E_1E_2\varepsilon + \eta(E_1 + E_2)\dot{\varepsilon} = E_2\sigma + \eta\dot{\sigma}. \tag{6}$$

For Figure 2(b):

$$E_1E_2\varepsilon + E_1\eta\dot{\varepsilon} = (E_1 + E_2)\sigma + \eta\dot{\sigma}. \tag{7}$$

Next, a series of substitutions are made to form the two corresponding constitutive relations for a rate-dependent CZM [14]: (1) across the cohesive zone, the opening displacement (Δu_n) and the cohesive surface traction (T_n) are used to replace strain (ε) and stress (σ) in the models, respectively; (2) the stiffness of the rate-independent CZM is used to replace E_1 in the model; (3) a constant η_n with a unit of force per velocity per area is used to replace the viscosity coefficient η to describe the cohesive zone viscosity; (4) a secondary stiffness k_2 with a unit of force per relative displacement per area is used to replace the modulus, E_2. Consequently, the rate-dependent CZM can be established by combining a rate-independent CZM with a Maxwell element in parallel, or a rate-independent CZM with a Kelvin element in series. To distinguish them in the latter section, we simply define them as model A and model B, respectively.

Taking the normal separation into account, the constitutive behavior of model A can be rewritten in the following form [14]:

$$k_2\tilde{T}_n + \eta_n\left(\frac{\text{d}\tilde{T}_n}{\text{d}\Delta u_n} + k_2\right)\Delta\dot{u}_n = k_2T_n + \eta_n\dot{T}_n, \tag{8}$$

where the subscript n denotes the normal direction. $\tilde{T}_n$, which is proposed by Xu and Needleman [21], represents the traction of the rate-independent CZM:

$$\tilde{T}_n = T_{n\max}\exp\left(1-\frac{\Delta u_n}{\delta_n}\right)\left[\frac{\Delta u_n}{\delta_n} + \frac{1-q}{r-1}\left(r-\frac{\Delta u_n}{\delta_n}\right)\right], \tag{9}$$

where δ_n, q and r are constitutive parameters. $T_{n\max}$ is the maximum value of normal traction.

The constitutive relation of model B can be written as:

$$\frac{\text{d}\tilde{T}_n}{\text{d}\Delta\tilde{u}_n}k_2\Delta u_n + \eta_n\frac{\text{d}\tilde{T}_n}{\text{d}\Delta\tilde{u}_n}\Delta\dot{u}_n = \left(\frac{\text{d}\tilde{T}_n}{\text{d}\Delta\tilde{u}_n} + k_2\right)T_n + \eta_n\dot{T}_n, \tag{10}$$

where $\Delta\tilde{u}_n$ is the displacement of the rate-independent CZM.

3.2 Incrementation in the viscoelastic CZM

In an attempt to formulate the viscoelastic constitutive eqs.

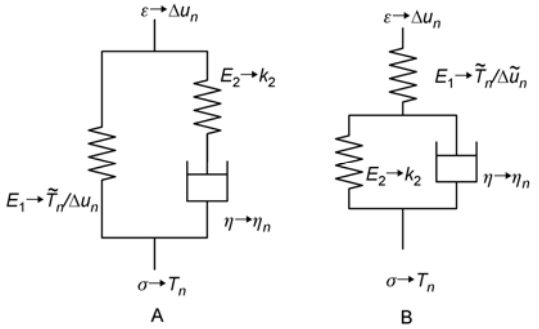

Figure 2 Linear solid viscoelastic model for rate-dependent CZM analysis.

(8) and (10) into a computational finite element model, it is necessary to increment the cohesive zone traction at each time step. For model A, suppose that the traction at time t is known and that the traction at $t+\Delta t$ is evaluated as follows [15]:

$$T_n(t+\Delta t) = \tilde{T}_n(t+\Delta t) + \frac{E_2[\Delta u_n(t+\Delta t) - \Delta u_n(t)] + T_n(t) - \hat{T}_n(t)}{1 + k_2 \Delta t / \eta}. \quad (11)$$

Based on viscoelastic theory, the tractions associated with the rate-independent CZM and the Kelvin element are equal for model B, whereas the displacements are additive. Hence, eq. (10) can be written as:

$$T_n = \tilde{T}_n, \quad (12)$$

$$T_n = k_2 \Delta u_2 + \eta_n \Delta \dot{u}_2, \quad (13)$$

$$\Delta u_n = \Delta \tilde{u}_n + \Delta u_2, \quad (14)$$

where u_2 is the displacement of the Kelvin model. Substituting eqs. (12) and (14) into eq. (13), a linear first-order differential equation is given as follows:

$$\tilde{T}_n = k_2(\Delta u_n - \Delta \tilde{u}_n) + \eta_n(\Delta \dot{u}_n - \Delta \dot{\tilde{u}}_n). \quad (15)$$

To ensure accuracy and stability of the solution, here the modified Euler method is chosen to solve $\Delta \tilde{u}_n$ in eq. (15). Then, T_n can be obtained based on eq. (12).

4 Numerical examples and discussion

4.1 Rate-dependent cohesive model

In order to observe how the rate-dependent CZM performs, several special cases are considered here. The effect of a monotonically increasing opening displacement up to failure is examined for a single element. The initial stiffness of the rate-independent CZM is $k_1 = \tilde{T}_{\max} \exp(1)/\delta_n$, and set k_2=0.02k_1 and k_2=0.2k_1 for model A and model B, respectively.

Figure 3 shows the curves of traction-separation at different separation rates v_n= 1, 0.1, 0.01 and 0.001. As can be seen, for low v_n the traction of the Maxwell element can be ignored. Therefore, the rate-dependent CZM behaves in the same way as the original rate-independent CZM. For large v_n the upper limit of the traction-separation curve approximates the rate-independent CZM model in parallel with the spring E_2 due to the inadequate viscous response in the short period of time. With v_n increasing, the peak traction shifts towards larger values: i.e., the cohesive strength is dependent on the loading rate. In the present model, the work of separation is not constant; namely, the cohesive energy increases with increasing loading rate, as illustrated in Figure 3. Contrarily, in the rate-independent CZM, the area under the traction displacement curve is a constant.

Figure 4 shows the traction-separation curves of model B for different v_n. As can be seen, with the decrease of v_n the curve changing tendency (which is different from model A) is from the original rate-independent CZM towards the rate-independent CZM model in series with the spring E_2. For different v_n, the peak traction remains unchanged: i.e., the cohesive strength is not affected by the loading rate. Finally, the variety of the cohesive energy is not monotonically increased with increasing v_n.

Consequently, the results show that it is necessary to choose an appropriate model for different viscoelastic materials. Most literature mentions that fracture toughness increases with increasing crack opening velocity; however, the variation of the fracture toughness is a complex function related to velocity [22]. Hence, both the constitutive relations of model A and model B are implemented into the finite element procedure to study the influence of the viscoelastic interfacial cracks on sandwich structures.

4.2 Double cantilever beam

4.2.1 Numerical model

Figure 5 shows a sandwich Double Cantilever Beam (DCB)

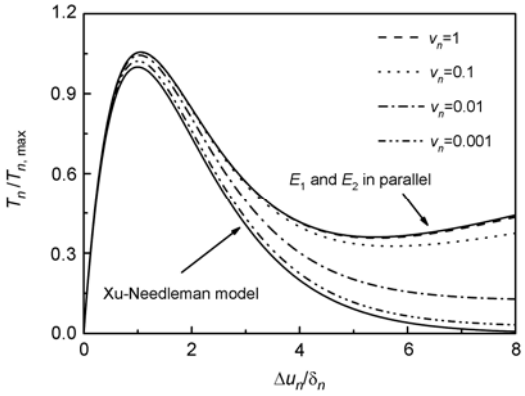

Figure 3 Traction-separation of model A for various loading rates.

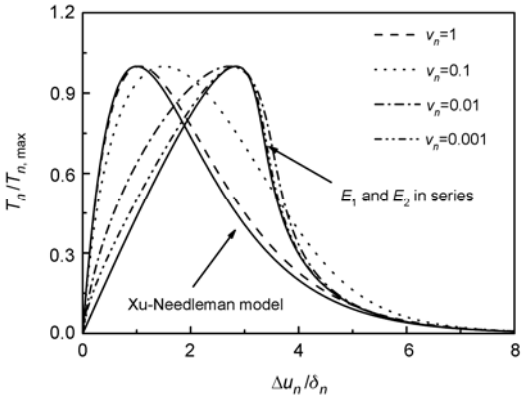

Figure 4 Traction-separation of model B for various loading rates.

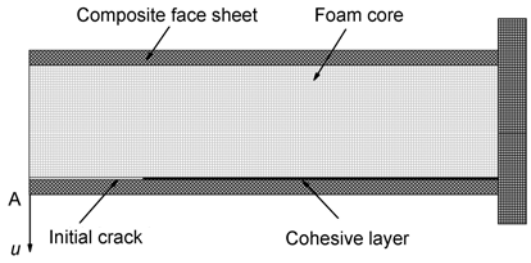

Figure 5 A sandwich Double Cantilever Beam (DCB) specimen with interface crack.

specimen with an initial interface crack between the lower face sheet and core. The lengths of specimen and crack are 210 mm and 50 mm, respectively, and the thicknesses of core and face sheet are 30 mm and 3.6 mm, respectively. The loading is imposed by the displacement u at point A in the lower face sheet, while the corresponding reaction force can be obtained from calculations.

Table 1 lists the mechanical materials properties of the face sheets and foam core. The material of the adhesive layers is complex because of the physical and chemical interaction in the fabrication process. This paper focuses on the fracture mechanisms analysis, so the material parameters of the adhesive layers are specified as in Table 2 corresponding to the experimental results in refs. [15,23].

For the analysis of the delamination propagation in sandwich structure beams, a detailed finite element discretization for a cross-section along the x-y plane is employed. The CZM described above is implemented in conjunction with the ABAQUS user element subroutine (UEL) [24]. For the sake of simplicity, all analyses are based on the plane strain condition. An initial crack is inserted into the interface between the lower face and core. Both the core and the two face sheets are discretized by four-node plane strain elements. The specimen consists of 4320 elements and 4561 nodes, as shown in Figure 6. The cohesive elements are placed along the interface between the face sheet and the core to capture the interfacial crack growth in the sandwich beams.

Table 1 Mechanical properties of materials [9]

Material property	E_x, E_y, E_z (GPa)	v_{xy}, v_{xz}, v_{yz}	G_{xy}, G_{xz}, G_{yz} (GPa)
Face sheet	24.6, 11.8, 13.5	0.31, 0.533, 0.446	3.78, 9.19, 3.74
Core	0.165, 0.263, 0.165	0.37, 0.37, 0.37	0.15, 0.15, 0.15

Table 2 Parameters related to rate-dependent CZM for DCB specimen

$T_{n\max}$ (MPa)	δ_n	G_c (N/mm)	q	r	η_n (MPa s/mm)
6	0.084	1.27	1	0	12.5

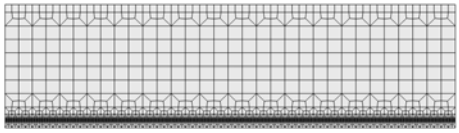

Figure 6 Finite element model of the DCB sandwich specimen.

4.2.2 *Validity of the numerical model*

To verify the validity of the present numerical model, let the material properties of the core and face sheets be the same as in Table 1. The rate-independent bilinear and Xu-Needleman laws of CZMs are employed in this section. The finite element mesh configuration is the same as that in Figure 6, excepting the boundary condition that the upper face sheet be fixed.

Figure 7 shows the variations of reaction force with tip displacement. The black dots are the experimental results. The solid curve and dashed curve represent the numerical results based on the bilinear law and the Xu-Needleman law, respectively. It can be seen that the reaction force P decreases with displacement u, increasing when the interface damage and crack growth occur, and the present numerical results agree well with the experimental results. Hence, it can be deduced that the numerical results are significantly affected by the cohesive energy, but not by the shape of the traction-separation curve.

4.2.3 *Effects from loading rates*

Here the effects when the sandwich DCB is subjected to different constant loading rates are considered. Model A is employed to characterize the viscoelastic behavior of the adhesive layer. The curves of the reaction force versus the tip displacement are shown in Figure 8, where the solid, dashed and dotted curves represent three loading rates: 2 mm/s, 0.2 mm/s and 0.02 mm/s, respectively. As mentioned in the previous section, cohesive energy is the main factor. Therefore, before the crack grows, the effects of the loading rates are not evident from the curves. Also, both the peak load and corresponding displacements increase with increasing loading rates: this illustrates that sandwich beam behavior toughens as loading rate increases. These conclusions are consistent with those of refs. [12,25].

The crack growth happens when the separation work of the cohesive element attains material toughness. Figure 9 shows the curves of crack growth length vs. displacement for three loading rates. Firstly, it can be found that for the

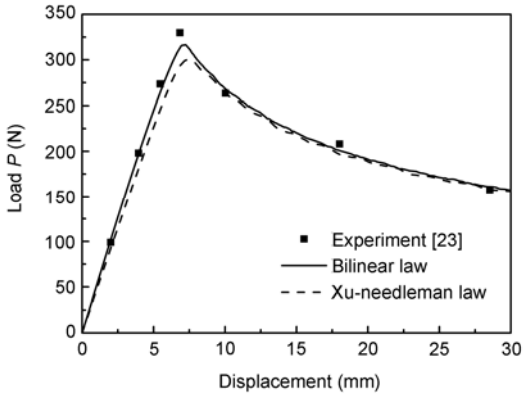

Figure 7 Load-displacement curves of numerical results and experimental results.

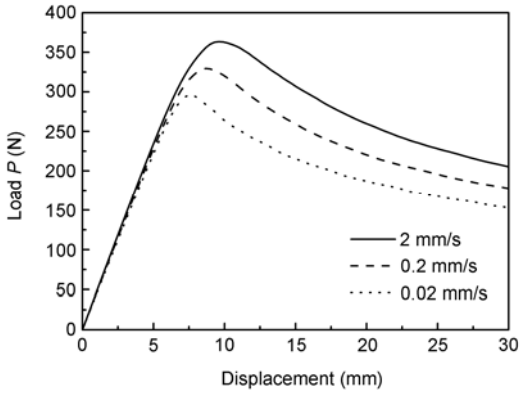

Figure 8 Load-displacement curves of DCB with model A for various loading rates.

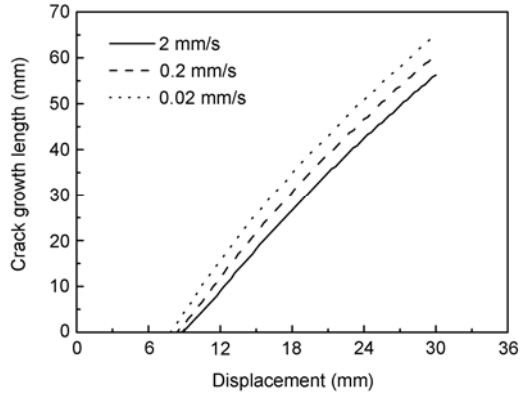

Figure 9 Crack growth Length vs. displacement curves of DCBs with model A for various loading rates.

crack onset the displacement needs to reach a certain value, the value of which increases with increasing loading rates. The reason is that forming the cohesive zone needs time for damage to accumulate. Secondly, with the loading rate decreasing, the crack growth length increases. This is due to the fact that the slow loading rate gives more time for damage evolution, and that the interface stress also has sufficient time to relax in the cohesive zone. Thus, the energy required for crack growth decreases as well.

The curves of the reaction force versus the loading displacement of DCBs with model B are shown in Figure 10. It can be seen that the peak load is increasing with loading rate: increasing from 0.02 mm/s to 2 mm/s, which is similar to the results from model A. However, the load vs. displacement curve presents a descent in the case of a higher loading rate (20 mm/s). This phenomenon indicates that interfacial toughness is decreasing, which is also described by the ref. [26].

5 Conclusions

Two rate-dependent CZMs, which characterize viscoelastic

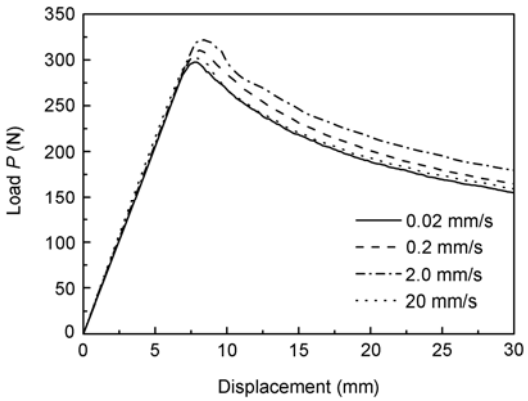

Figure 10 Load-displacement curves of DCBs with Model B for various loading rates.

behaviors within the fracture process zone ahead of the crack tip, have been employed for interfacial fracture analysis of composite sandwich beams. Through parametric analysis and discussion, the following conclusions have been reached:

(1) The rate-dependent CZM can be obtained by combining a rate-independent CZM with other viscoelastic elements such as a Maxwell element or a Kelvin element. Different combinations have influence on cohesive zone strength and energy under various loading rates.

(2) The viscoelastic constitution of the adhesive layer is represented by rate-dependent CZMs. The critical energy for crack growth is not a constant value for the different rate-dependent CZMs. For rate-independent CZMs and a Maxwell element in parallel, the sandwich beams exhibit more toughness as the face/core interfacial crack growth increases with an increasing loading rate. While for rate-independent CZMs and a Kelvin element in series, the variation of the interfacial toughness decreases with an increasing loading rate. It is necessary to consider rate-dependent effects caused by the viscoelastic characteristics of the interface on the fracture behavior of the sandwich material.

(3) Through reasonable optimization of material parameters for the viscoelastic layer, the fracture toughness of a composite sandwich can be improved, and hence its fracture resistance can be enhanced.

For lack of experimental data on rate-dependence of interface mediums, cohesive parameters are difficult to calibrate under higher loading rate conditions. The effects of the loading rate on the fracture toughness of the sandwich interface need to be studied further both experimentally and numerically.

The authors are grateful to Profs. Wang J X, Hu X Z and the anonymous referees for very helpful comments, which greatly improved the work. This work was supported by the National Natural Science Foundation of China (Grant Nos. 10672027 and 90816025) and the National Basic Research Program of China (Grant No. 2006CB601205).

1 Kim J K, Yu T X. Forming and failure behaviour of coated, laminated and sandwiched sheet metals: a review. J Mater Process Technol, 1997, 63: 33–42
2 Vadakke V, Carlsson L A. Experimental investigation of compression failure of sandwich specimens with face/core debond. Compos Part B, 2004, 35: 583–590
3 Avilés F, Carlsson L A. Analysis of the sandwich DCB specimen for debond characterization. Eng Fract Mech, 2008, 75: 153–168
4 Siriruk A, Penumadu D, Weitsman Y J. Effect of sea environment on interfacial delamination behavior of polymeric sandwich structures. Compos Sci Technol, 2009, 69: 821–828
5 Dugdale D S. Yielding of steel sheets containing slits. J Mech Phys Solids, 1960, 8: 100–104
6 Barenblatt G I. The mathematical theory of equilibrium cracks in brittle fracture. Adv Appl Mech, 1962, 7: 55–129
7 Elices M, Guinea G V, Gómez J, et al. The cohesive zone model: advantages, limitations and challenges. Eng Fract Mech, 2002, 69: 137–163
8 Elmarakbi A M, Hu N, Fukunaga H. Finite element simulation of delamination growth in composite materials using LS-DYNA. Compos Sci Technol, 2009, 69: 2383–2391
9 Sridharan S, Li Y. Static and dynamic delamination of foam core sandwich members. AIAA J, 2006, 44: 2937–2948
10 Han T S, Ural A, Chen C S, et al. Delamination buckling and propagation analysis of honeycomb panels using a cohesive element approach. Int J Fract, 2002, 115: 101–123
11 Bažant Z P, Li Y N. Cohesive crack with rate-dependent opening and viscoelasticity: I. Mathematical model and scaling. Int J Fract, 1997, 86: 247–265
12 Allen D H, Searcy C R. A micromechanical model for a viscoelastic cohesive zone. Int J Fract, 2001, 107: 159–176
13 Wu Y Q, Huang F L. A micromechanical model for predicting combined damage of particles and interface debonding in PBX explosives. Mech Mater, 2009, 41: 27–47
14 Xu C, Siegmund T, Ramani K. Rate-dependent crack growth in adhesives: I. Modeling approach. Int J Adhes Adhes, 2003, 23: 9–13
15 Xu C, Siegmund T, Ramani K. Rate-dependent crack growth in adhesives II. Experiments and analysis. Int J Adhes Adhes, 2003, 23: 15–22
16 Zhu Y, Liechti K M, Ravi-Chandar K. Direct extraction of rate-dependent traction-separation laws for polyurea/steel interfaces. Int J Solids Struct, 2009, 46: 31–51
17 Cornec A, Scheider I, Schwalbe K. On the practical application of the cohesive model. Eng Fract Mech, 2003, 70: 1963–1987
18 Sun S Y, Chen H R. Quasi-static and dynamic fracture behavior of composite sandwich beams with a viscoelastic interface crack. Compos Sci Technol, 2010, 70: 1011–1016
19 Mi Y, Crisfield M A, Davies G A O, et al. Progressive Delamination Using Interface Elements. J Compos Mater, 1998, 32: 1246–1272
20 Ortiz M, Pandolfi A. Finite-deformation irreversible cohesive elements for three-dimensional crack-propagation analysis. Int J Numer Meth Eng, 1999, 44: 1267–1282
21 Xu X P, Needleman A. Numerical simulations of fast crack growth in brittle solids. J Mech Phys Solids, 1994, 42: 1397–1434
22 Makhecha D P. Dynamic Fracture of Adhesively Bonded Composite Structures Using Cohesive Zone Models. Dissertation for the Doctoral Degree. Virginia: Virginia Polytechnic Institute and State University, 2005
23 Li X M, Carlsson L A. Elastic foundation analysis of tilted sandwich debond (TSD) specimen. J Sandwich Struct Mater, 2000, 2: 3–32
24 Hibitt, Karlsson & Sorenson, Inc. ABAQUS User's Manual Version 6.4, 2004
25 Wang J, Kang Y L, Qin Q H, et al. Identification of time-dependent interfacial mechanical properties of adhesive by hybrid/inverse method. Comp Mater Sci, 2008, 43: 1160–1164
26 Papanicolaou G C, Bakos D. Interlaminar fracture behaviour of sandwich structures. Compos Part A, 1996, 27: 165–173